Finite-size scaling in the transverse Ising model on a square lattice

2000 J. Phys. A: Math. Gen. 33 6683

(http://iopscience.iop.org/0305-4470/33/38/303)

J. Phys. A: Math. Gen. **33** (2000) 6683–6698. Printed in the UK PII: S0305-4470(00)15502-7

Finite-size scaling in the transverse Ising model on a square lattice

C J Hamer

School of Physics, University of New South Wales, Sydney, NSW 2052, Australia

E-mail: c.hamer@unsw.edu.au

Received 5 July 2000

Abstract. Energy eigenvalues and order parameters are calculated by exact diagonalization for the transverse Ising model on square lattices of up to 6×6 sites. Finite-size scaling is used to estimate the critical parameters of the model, confirming universality with the three-dimensional classical Ising model. Critical amplitudes are also estimated for both the energy gap and the ground-state energy.

1. Introduction

Recent advances in computer technology have allowed the exact diagonalization of Ising-type quantum spin systems of up to 36 sites in size. Schulz *et al* (1996), for example, studied the J1-J2 XXZ Heisenberg spin model on square lattices with up to 6×6 sites. Our aim in this paper is to carry out an exact diagonalization study of the transverse Ising model on the square lattice, in order to estimate its critical parameters and study its finite-size scaling behaviour.

The transverse Ising model in (2 + 1)D is well known to be the quantum Hamiltonian corresponding to the classical 3D Ising model (Suzuki 1976, Fradkin and Susskind 1978), and exhibits a quantum phase transition in the same universality class as the classical 3D Ising thermal transition. It was first studied by series expansion methods by Pfeuty and Elliott (1971), and there have been several further series expansion calculations since then, both 'low temperature' (Yanase *et al* 1976, Marland 1981, Oitmaa *et al* 1991) and 'high temperature' (Hamer and Irving 1984, Hamer and Guttmann 1989, He *et al* 1990). Exact finite-lattice calculations have also been carried out previously (Roomany and Wyld 1980, Hamer 1983, Henkel 1984, 1987) for square lattices of up to 5×5 sites, and similar calculations have also been done for the triangular lattice (Hamer and Johnson 1986, Henkel 1990, Price *et al* 1993). Here we extend these calculations for the first time to the 6×6 lattice, and use finite-size scaling theory to obtain improved estimates of the critical point and critical index ν. Recently, a density matrix renormalization group (DMRG) calculation has been carried out for this model on lattices up to 30×6 sites in size by de Jongh and van Leeuwen (2000), but the accuracy of these calculations is not yet sufficient to rival Monte Carlo simulations.

The finite-size scaling amplitudes at the critical point are also of interest. In (1 + 1)D, it is well known that the theory of conformal invariance relates the scaling amplitudes to fundamental parameters of the underlying effective field theory at the critical point, such as the conformal anomaly and scaling indices. In higher dimensions, a similar scenario is known to hold at 'first-order' transitions, where a continuous symmetry is spontaneously broken, giving

0305-4470/00/386683+16$30.00

rise to Goldstone bosons (Hasenfratz and Leutwyler 1990): the finite-size scaling amplitudes are related to parameters of the Goldstone bosons such as the spin-wave stiffness and spin-wave velocity. Does something similar apply at second-order transitions in higher dimensions? Apart from a discussion by Cardy (1985), little has been done in this area. One peculiar result was obtained by Henkel (1986, 1987) and Weston (1990), and confirmed recently by Weigel and Janke (1999): the scaling amplitudes of the spin–spin and energy–energy correlation lengths on *antiperiodic* lattices have a universal ratio

$$\frac{A_\sigma}{A_\epsilon} = \frac{x_\sigma}{x_\epsilon} \tag{1.1}$$

where the x_i are the scaling indices in the respective sectors. This phenomenon appears to have no good theoretical explanation at the present time.

Our exact diagonalization methods are outlined briefly in section 2, and the numerical results are presented in section 3. The critical parameters so obtained are compared with other estimates in table 5 of section 4, and the critical amplitudes are also discussed there.

2. Method

The transverse Ising model on the square lattice has the Hamiltonian

$$H = \sum_i (1 - \sigma_3(i)) - x \sum_{\langle ij \rangle} \sigma_1(i)\sigma_1(j) - h \sum_i \sigma_1(i) \tag{2.1}$$

where the sum $\langle ij \rangle$ runs over nearest neighbour pairs on the lattice, and the σ matrices are the usual Pauli spin operators acting on a 2-state spin-variable at each site. The coupling x is analogous to an inverse 'temperature', and h represents an external 'magnetic field'. We shall employ a representation in which the $\sigma_3(i)$ are diagonal. Periodic boundary conditions are assumed.

The unperturbed ground state of the model at $x = 0$ has all spins 'up', i.e. $\sigma_3(i) = +1$, for all i. The interaction term will induce an admixture of states with 'flipped' spins. The Hilbert space of the model consists of two sectors, containing an odd and even number of flipped spins respectively.

Exact diagonalizations have been carried out for $L \times L$ lattices, $L = 1, \ldots, 6$. The methods employed are fairly standard, for the most part, and will not be described in detail here. First, a list of allowed basis states in the given sector was prepared, using the 'sub-lattice coding' technique of Lin (1990). This efficient technique produces a sorted list of states, requiring only one integer word of storage per state. Since only the zero-momentum states are considered here, the states were 'symmetrized', that is, all copies of a given state under translations, reflections and rotations were represented by a single state. Thus, for the 6×6 lattice in the even sector, the total number of 'unsymmetrized' states is approximately 2^{35}, whereas under symmetrization this is reduced by a factor of approximately 288, down to 119, 539, 680.

Next, the Hamiltonian matrix elements are generated, by applying the interaction operators of equation (2.1) to each initial state, symmetrizing the resulting final state, and looking it up in the master file. The elements were grouped into blocks, each of which acts between small subsets of the initial- and final-state vectors, to avoid 'thrashing' during the matrix multiplications. Within each subset, the initial and final addresses can each be fitted into a half-integer, so that the matrix elements occupied 35 Gbyte of storage over all.

Finally, the lowest eigenvalue and eigenvector of the Hamiltonian were found in each sector, using the conjugate gradient method. Nightingale *et al* (1993) showed that the conjugate gradient method converges faster than the Lanczos method for large problems such as this. We

found that the eigenvalue converged to an accuracy of one part in 10^{10} in 20–25 iterations for the 6×6 lattice in the neighbourhood of the critical point.

Having determined the quantities of interest for each finite lattice, it is then necessary to make an extrapolation to $L \to \infty$, to estimate the bulk behaviour of the system. In the vicinity of the critical point, the finite-lattice sequence will typically behave as

$$f_L = f_\infty + a_1 L^{-\omega_1} + a_2 L^{-\omega_2} + \cdots \tag{2.2}$$

where the ω_i are non-integer exponents, in general (Barber 1983). The problem of extrapolating such a sequence has been discussed in several reviews (Barber and Hamer 1982, Smith and Ford 1982, Guttmann 1989). We have employed a number of different algorithms, including:

(i) the Neville table (Guttmann 1989), which is best suited to a simple polynomial sequence, with integer exponents ω_i;
(ii) the alternating VBS algorithm (van den Broeck and Schwartz 1979, Barber and Hamer 1982), which can give good convergence for sequences of type (2.2), but needs at least two iterations to work well;
(iii) the Lubkin algorithm (1952), which is more suitable for short sequences;
(iv) the Bulirsch–Stoer (1964) algorithm, which has been applied in this context by Henkel and Patkos (1987), and Henkel and Schütz (1988). This algorithm involves an explicit parameter ω which can be optimized to match the leading power-law correction. It has been claimed by Henkel and Schütz (1988) that the algorithm is more robust and more accurate than the VBS algorithm, especially for short sequences.

3. Results

3.1. Finite-lattice data

The pseudo-critical point at lattice size L can be defined according to finite-size scaling theory (Barber 1983) as the coupling x_L such that

$$R_L(x_L) = 1 \tag{3.1}$$

where $R_L(x)$ is the scaled energy-gap ratio

$$R_L(x) = \frac{L F_L(x)}{(L-1) F_{L-1}(x)} \tag{3.2}$$

and $F_L(x)$ is the energy gap for lattice size L. This point is found by calculating the energy eigenvalues at a cluster of five equally spaced points in the neighbourhood of x_L, and then finding x_L by interpolation between them. The spacing between the points was chosen as $\Delta x = 0.001$, estimated to balance the truncation and round-off errors in the calculation. The values of all other observables can then be estimated at x_L by the same finite-difference interpolation procedures. Tables 1 and 2 list the pseudo-critical points x_L, and the values of the calculated observables at coupling x_L for each pair of lattice sizes L and $(L-1)$, for $L = 2$–6. The values of x_L for $L = 2$–5 listed in table 1 agree through to six figures with those calculated previously (Hamer 1983).

Table 1 lists values for the ground-state energy per site $\epsilon_{0,L}$ for lattice size L, and its derivatives $\epsilon'_{0,L}$ and $\epsilon''_{0,L}$, where the prime denotes differentiation with respect to x. The values are expected to be accurate to the figures quoted (or better) as regards round-off error. The truncation error in the five-point interpolation process is harder to estimate, since it involves unknown higher derivatives of ϵ_0, but we estimate it should be no more than about one part in 10^{12} for ϵ_0 and one part in 10^6 for ϵ''_0.

Table 1. Finite-lattice data at the pseudo-critical points x_L, calculated for the pair of lattice sites L and $(L-1)$ in each case. The ground-state energy per site ϵ_0, its first two derivatives ϵ_0' and ϵ_0'' with respect to x, and the susceptibility χ are given.

x_L	L	ϵ_0	ϵ_0'	ϵ_0''	χ
0.260 342 382 22	1	−0.520 684 764 436	−2.000 000 00	0.000 00	−1.000 00
	2	−0.074 060 535 180	−0.611 632 73	−2.908 81	−3.628 4
0.316 000 087 72	2	−0.112 709 188 696	−0.778 665 08	−3.069 19	−5.041 49
	3	−0.070 818 161 984	−0.598 797 39	−4.151 19	−11.214 3
0.324 249 252 29	3	−0.075 901 188 836	−0.633 841 13	−4.343 70	−12.575 2
	4	−0.066 430 308 096	−0.571 145 18	−5.099 31	−22.204 9
0.326 695 938 06	4	−0.067 843 120 636	−0.583 789 35	−5.236 41	−23.542 6
	5	−0.064 637 823 298	−0.552 955 27	−5.833 24	−36.578 8
0.327 583 267 52	5	−0.065 130 784 765	−0.558 170 35	−5.921 35	—
	6	−0.063 752 757 694	−0.540 125 09	−6.420 27	—

Table 2. Finite-lattice data as in table 1, consisting of the mass gap F_L, its first two derivatives F_L' and F_L'' with respect to x, and the 'magnetization' M_L.

x_L	L	F_L	F_L'	F_L''	M_L
0.260 342 382 22	1	2.000 000 000 000	0.000 0000	0.000 00	1.000 00
	2	1.000 000 000 000	−3.400 7921	6.052 94	0.673 37
0.316 000 087 72	2	0.820 891 162 135	−3.022 3297	7.444 33	0.719 08
	3	0.547 260 774 756	−4.469 5972	13.956 4	0.583 57
0.324 249 252 29	3	0.510 885 529 302	−4.347 0817	15.741 6	0.597 05
	4	0.383 164 146 983	−5.408 8281	25.060 3	0.515 20
0.326 695 938 06	4	0.370 007 329 425	−5.345 2110	26.945 0	0.521 30
	5	0.296 005 863 592	−6.233 7554	39.389 6	0.464 88
0.327 583 267 52	5	0.290 490 201 648	−6.198 0387	41.116 7	—
	6	0.242 075 167 8	−6.985 0090	56.763 6	—

We have also listed values in table 1 for the magnetic susceptibility, defined by

$$\chi_L = -\frac{1}{L^2}\left.\frac{\partial^2 E_{0,L}(x,h)}{\partial h^2}\right|_{h=0}. \tag{3.3}$$

This derivative was also estimated by a finite difference method, using a cluster of five data points around $h = 0$, with a spacing $\Delta h = 0.0003$, giving an estimated truncation error of no more than one part in 10^6 in the susceptibility. This calculation was a little too large to carry through for $L = 6$, with the facilities available.

Table 2 lists the energy gap F_L between the odd and even sectors, and its derivatives F_L' and F_L'', at each x_L. Values are also listed here for the quantity M_L defined by

$$M_L = \langle 0|\sigma_1(1)|1\rangle \tag{3.4}$$

where $|0\rangle$, $|1\rangle$ are the lowest lying energy eigenvectors in the even and odd sectors, respectively. It can be shown (Yang 1952, Uzelac 1980, Hamer 1982) that this quantity converges towards the spontaneous magnetization in the bulk limit. Unfortunately, for technical reasons, we were again unable to calculate this quantity for $L = 6$. Since the accuracy of the wavefunction is only the square root of that of the eigenvalue, the round-off error in these values is expected to be about one part in 10^6.

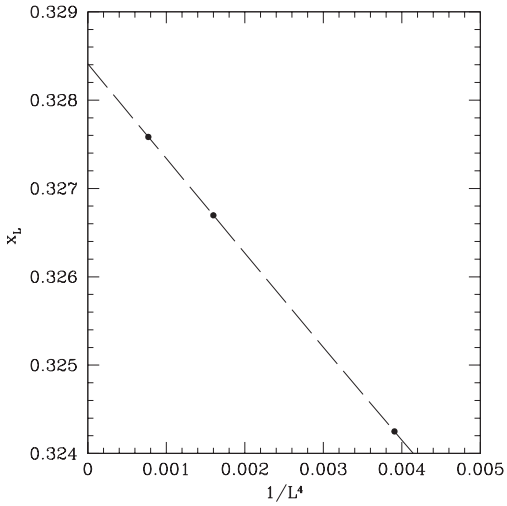

Figure 1. Graph of the finite-lattice pseudo-critical points x_L as a function of $1/L^4$. The line is merely to guide the eye.

3.2. Critical point

The sequence of pseudo-critical points x_L converges rapidly, as can be seen in figure 1, where x_L is plotted against $1/L^4$. To estimate the bulk limit ($L \to \infty$) of this sequence, we have employed various algorithms discussed above, as well as a simple polynomial fit in $1/L^4$ and higher powers.

Our final estimate of the critical point is

$$x_c = 0.328\,41(2). \tag{3.5}$$

This is consistent with our earlier finite-size estimate of $x_c = 0.3289(10)$ (Hamer 1983), but nearly two orders of magnitude more accurate. Henkel (1987) obtained an improved estimate $x_c = 0.3282(1)$ from lattices with up to 5×5 sites.

3.3. Critical indices

Finite-size scaling theory (Barber 1983) also tells us how to estimate the critical indices for the model. The finite-lattice susceptibility χ_L, for instance, is predicted to scale at the critical point as

$$\chi_L(x_c) \sim L^{\gamma/\nu} \qquad L \to \infty \tag{3.6}$$

and hence one finds that

$$L\left(1 - \frac{\chi_L(x_L)}{\chi_{L-1}(x_L)}\right) \sim -\frac{\gamma}{\nu} \qquad L \to \infty. \tag{3.7}$$

Similarly, ratios of the finite-lattice 'magnetizations' (equation (3.4)) give estimates of β/ν. Finally, estimates of the index $1/\nu$ can be obtained from the Callan–Symanzik 'beta function' (Barber 1983)

$$\beta_L(x)/g = \frac{F_L(x)}{(F_L(x) - 2xF_L'(x))} \tag{3.8}$$

Table 3. Finite-size scaling estimates of the critical indices, as defined by equation (3.7) and the text which followed, where L is the larger of the two lattice sizes used in the estimate.

L	$1/\nu$	$1-\alpha/\nu$	β/ν	γ/ν	p
2	1.278 17	—	0.653 264	1.448 80	—
3	1.380 21	1.884 08	0.565 352	1.651 32	1.718 62
4	1.432 42	1.206 61	0.548 326	1.734 69	2.095 67
5	1.463 77	1.050 69	0.541 083	1.781 95	2.307 81
6	1.484 79	0.984 36	—	—	2.420 47
∞	1.591(2)	0.84(1)	0.523(2)	1.95(1)	2.8(2)

Table 4. 'Logarithmic' finite-size scaling estimates of the critical indices, as defined by equation (3.12) and the text which followed, where L is the larger of the two lattice sizes used in the estimate.

L	$1/\nu$	$1-\alpha/\nu$	β/ν	γ/ν	p
2	—	—	—	—	—
3	1.520 02	2.439 01	0.514 989	1.971 78	4.836 867 09
4	1.541 05	1.248 04	0.512 493	1.976 42	4.168 378 15
5	1.552 26	1.057 15	0.513 266	1.974 79	3.855 246 95
6	1.559 37	0.982 87	—	—	3.630 017 74
∞	1.593(3)	0.84(1)	0.521(3)	1.96(1)	2.5(2)

via

$$L\left(1-\frac{\beta_L(x_L)}{\beta_{L-1}(x_L)}\right)\sim\frac{1}{\nu}\qquad L\to\infty. \tag{3.9}$$

One would expect to obtain estimates of the ratio α/ν in a similar fashion from the 'specific heat'

$$C_L(x)=-\frac{x^2}{L^2}\frac{\partial^2\epsilon_0}{\partial x^2} \tag{3.10}$$

but it is known (Hamer 1983) that these estimates are very poor; too high by a factor of nearly 2. The reason is easily found: the ground-state energy or specific heat contains a 'regular' or analytic piece as well as the singular term (Privman and Fisher 1984). Henkel (1987) has cleverly sidestepped this problem, using a transition amplitude to find α/ν, in analogy to equation (3.4). Here, we eliminate the regular term by subtracting

$$\epsilon''_{0,L}-\epsilon''_{0,L-1}\sim L^{\alpha/\nu-1}\qquad L\to\infty \tag{3.11}$$

and using successive ratios of these differences to estimate $1-\alpha/\nu$. The estimates so obtained for the critical index ratios are listed in table 3.

Alternatively, 'logarithmic' estimates of the critical indices may be obtained as follows:

$$\frac{\ln[\chi_L(x_L)/\chi_{L-1}(x_L)]}{\ln[L/(L-1)]}\sim\frac{\gamma}{\nu}\qquad L\to\infty. \tag{3.12}$$

These alternative estimates are listed in table 4. The finite-size corrections are generally smaller for the logarithmic estimates.

These finite-size estimates of the critical indices agree closely with the previous calculation of Hamer (1983) up to $L=5$; and, remarkably enough, most of them agree to within four significant figures with the equivalent results obtained for the triangular lattice (Hamer and Johnson 1986, Price *et al* 1993).

The same algorithms mentioned above have been employed to extrapolate these sequences to their bulk limit. The sequences are very short, and may have slight irregularities, so that the

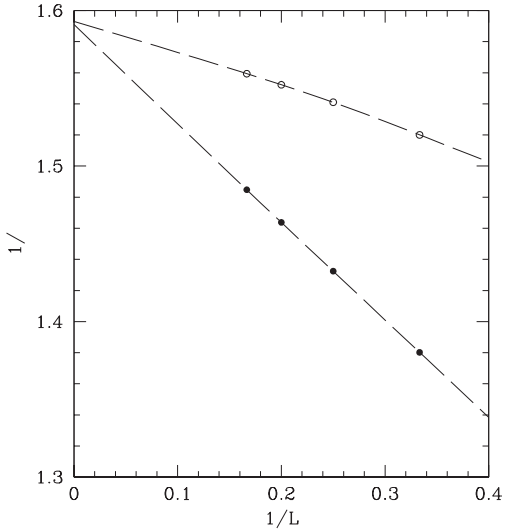

Figure 2. Finite-lattice estimates of the index $1/\nu$ plotted against $1/L$. The solid circles are 'linear' estimates, the open circles are 'logarithmic' estimates. The lines are merely to guide the eye.

tabular algorithms are generally no more accurate than simple graphical methods or polynomial fits in the extrapolation. The resulting estimates are listed at the foot of tables 3 and 4. The errors in these estimates are inevitably rather subjective, but the variation between different algorithms gives some indication of the likely error.

Figure 2 gives a graphical representation of the estimates of $1/\nu$ from tables 3 and 4 as a function of $1/L$: it can be seen that the behaviour is almost precisely linear for the estimates from table 3. Correspondingly, the Neville tables and polynomial fits give stable results, while the Lubkin and Bulirsch–Stoer algorithms give less stable results, possibly a little higher. We conclude that

$$\frac{1}{\nu} = 1.591(2). \tag{3.13}$$

The estimates for α/ν are not quite so well behaved, but our final estimate is

$$\frac{\alpha}{\nu} = 0.16(1). \tag{3.14}$$

This is a much better result than can be obtained directly from the specific heat, equation (3.10).

The estimates for the other indices β/ν and γ/ν are rapidly convergent, but we only have data up to $L = 5$ which were known previously. We find

$$\frac{\beta}{\nu} = 0.522(2) \tag{3.15}$$

$$\frac{\gamma}{\nu} = 1.96(1). \tag{3.16}$$

3.4. Energy amplitudes

The finite-size behaviour of the energy gap at the critical point is

$$F_L(x_L) \sim \frac{A_1}{L} \qquad L \to \infty \tag{3.17}$$

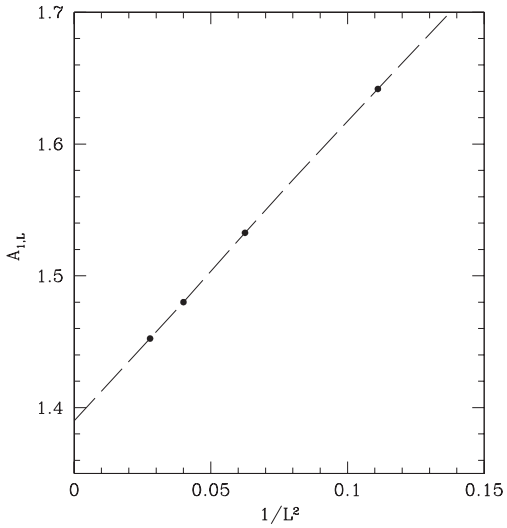

Figure 3. The energy gap amplitude $A_{1,L}$ plotted against $1/L^2$.

so the amplitude A_1 can be estimated by

$$LF_L(x_L) \sim A_1 \qquad L \to \infty. \tag{3.18}$$

The sequence of estimates for A_1 is shown in figure 3. It extrapolates to a value

$$A_1 = 1.39(1). \tag{3.19}$$

A value of 1.42 was previously estimated by Henkel (1987).

The finite-size scaling behaviour of the ground-state energy per site ϵ_0 at the pseudo-critical point is shown in figure 4. The finite-size scaling corrections appear to decrease as $1/L^3$, in accordance with the Privman–Fisher (1984) scaling hypothesis, which states that the singular part of the free-energy density of a system of finite size L should scale as L^{-d} (here $d = 3$). A polynomial fit on this assumption gives

$$\epsilon_{0,L}(x_L) \sim \epsilon_0^* - \frac{A_0}{L^3} \qquad L \to \infty \tag{3.20}$$

with

$$\epsilon_0^* = -0.624(1) \tag{3.21}$$

and

$$A_0 = 0.38(5). \tag{3.22}$$

Further evidence for this power-law behaviour can be obtained as follows. Suppose

$$\epsilon_{0,L}(x_L) \sim \epsilon_0^* - A_0/L^p \qquad L \to \infty \tag{3.23}$$

then

$$L\left[1 - \frac{(\epsilon_{0,L}(x_L) - \epsilon_{0,L-1}(x_L))}{(\epsilon_{0,L-1}(x_{L-1}) - \epsilon_{0,L-2}(x_{L-1}))}\right] \equiv p_L \sim p \qquad \text{as} \quad L \to \infty \tag{3.24}$$

and

$$\ln\left[\frac{\epsilon_{0,L}(x_L) - \epsilon_{0,L-1}(x_L)}{\epsilon_{0,L-1}(x_{L-1}) - \epsilon_{0,L-2}(x_{L-1})}\right] \Big/ \ln\left[\frac{L}{L-1}\right] \sim -p \qquad \text{as} \quad L \to \infty. \tag{3.25}$$

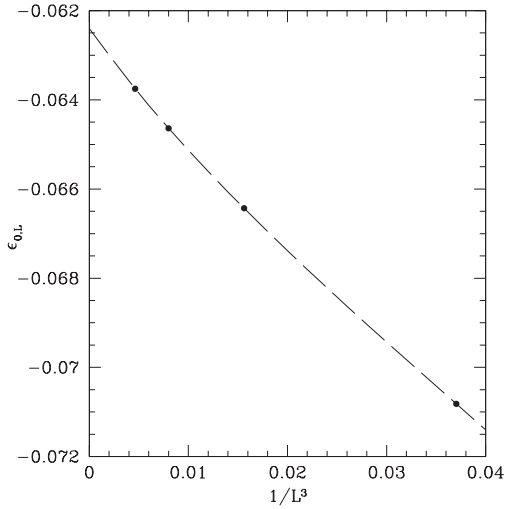

Figure 4. The ground-state energy per site at lattice size L plotted against $1/L^3$.

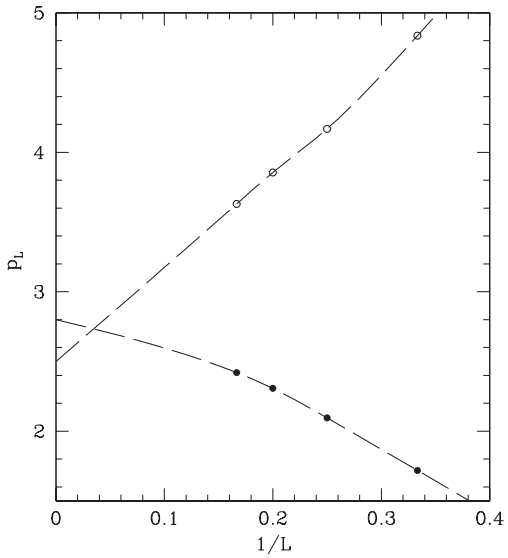

Figure 5. The effective exponent p_L plotted against $1/L$.

The sequences of finite lattice estimates for p are shown in figure 5. It can be seen that the 'linear' sequence comes down towards three from above, whilst the 'logarithmic' sequence comes up towards three from below. The sequences are a little irregular, however, and the best estimate we can obtain for the bulk limit is

$$p = 2.8(2), \tag{3.26}$$

a little lower than, but still consistent with, 3.

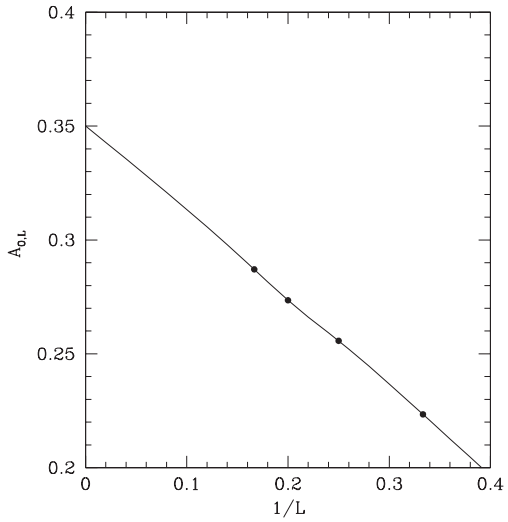

Figure 6. The Casimir amplitude $A_{0,L}$ plotted against $1/L$.

Assuming that $p = 3$, the scaling amplitude A_0 for the ground-state energy can be found by

$$\frac{L^4}{3}(\epsilon_{0,L}(x_L) - \epsilon_{0,L-1}(x_L)) \sim A_0 \qquad L \to \infty. \tag{3.27}$$

The sequence of estimates for A_0 is plotted in figure 6 and extrapolates to a value

$$A_0 = 0.35(2) \tag{3.28}$$

which is in reasonable agreement with equation (3.22). Henkel (1987) previously obtained an estimate of 0.39 for this quantity (allowing for the different normalization of his Hamiltonian). Mon (1985) obtained a Monte Carlo estimate of the corresponding free-energy amplitude in the 3D classical model.

In order to calibrate this result, we need to know the 'speed of light' v, or in other words the scale factor needed in this model to make the long-range correlations isotropic in space and time at the critical point. We have attempted to estimate this using the dispersion relation for the lowest excited state at the critical point, expected to be of the form

$$E(k) = vk \tag{3.29}$$

in the bulk system. We have calculated the finite-lattice eigenvalues for low-lying excited states with non-zero momentum for lattice sizes $L = 2$–5, and set

$$v_L = \frac{L}{2\pi}\left(F_L\left(x_L, \frac{2\pi}{L}\right) - F_L(x_L, 0)\right) \sim v \qquad L \to \infty \tag{3.30}$$

where $F_L(x, k)$ is the energy at coupling x for momentum k. Figure 7 shows the sequence of finite-lattice estimates for v as a function of $1/L$. They extrapolate to a bulk value

$$v = 0.99(3). \tag{3.31}$$

The ratio A_0/v should be a universal number, independent of the normalization of the Hamiltonian. From the results above, we find

$$\frac{A_0}{v} = 0.35(2) \tag{3.32}$$

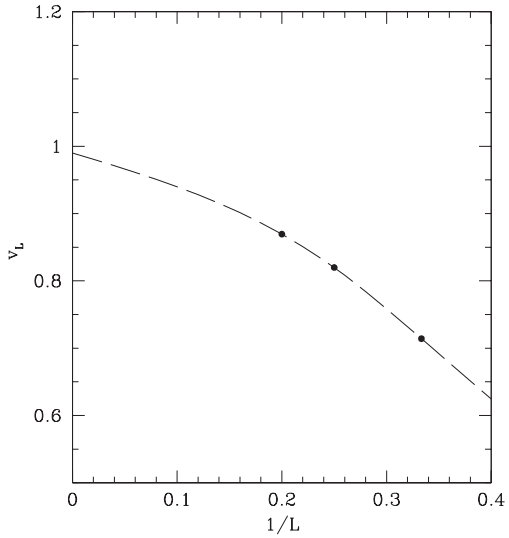

Figure 7. Finite-lattice estimates of the 'speed of light' v plotted against $1/L$.

which can be compared with values of 0.719 expected according to effective field theory for a single free boson (Hasenfratz and Niedermayer 1993), or 0.211 for a single free fermion degree of freedom (appendix). The result (3.31) matches neither of these values. This is not surprising, since the effective field theory at the critical point is expected to be a non-trivial interacting theory. It might be possible to estimate this quantity via the ϵ-expansion, using a Landau–Ginzburg effective field theory. This has not yet been done, as far as we are aware.

4. Conclusions

We have calculated the lowest-lying energy eigenvalues of the transverse Ising model on the square lattice with periodic boundary conditions for lattice sizes with up to 6×6 sites, using the conjugate gradient method. Finite-size scaling theory has been employed to estimate the critical parameters, which are compared with previous estimates in table 5.

It can be seen that our present estimates agree well with earlier finite-size scaling results. We have achieved a substantial increase in accuracy for the critical point, but only a more modest increase for the critical index ν. The results appear very compatible with previous series analyses, and also with recent estimates for the classical 3D Ising model and field theory. This provides further confirmation of the universality between these transitions. Finally, it can be seen that the accuracy of the exponents for the quantum model is now not very far behind that for the classical model.

We have also estimated the finite-size scaling amplitudes for the energy eigenvalues at the critical point. For the spin gap we find

$$A_1 = 1.39(1) \tag{4.1}$$

which can be compared with a previous estimate by Henkel (1987) of $A_1 = 1.42$.

For the ground-state energy, we have presented evidence that

$$\epsilon_{0,L}(x_L) \sim \epsilon_0^* - \frac{A_0}{L^3} \qquad L \to \infty \tag{4.2}$$

Table 5. A comparison of critical parameters obtained in this paper with some others obtained elsewhere. Key: HT = high-temperature series; LT = low-temperature series; FS = finite-size scaling; MC = Monte Carlo; TR = triangular lattice; SQ = square lattice.

	ν	α	β	γ	x_c
	(2 + 1)-dimensional Ising model				
FS SQ Hamer (1983)	0.635(5)				0.328 9(10)
FS SQ Henkel (1984, 1987)	0.629(2)	0.11(1)	0.324(9)	—	0.328 2(1)
FS SQ This work	0.629(1)	0.10(1)	0.328(2)	1.23(1)	0.328 41(2)
FS TR Hamer and Johnson (1986)	0.627(4)	—	0.332(6)	1.236(8)	
FS TR Price *et al* (1993)	0.627(2)	0.12(2)	0.324(3)	1.23(1)	
HT SQ He *et al* (1990)	0.637(4)	0.11(2)		1.244(4)	0.328 51(8)
LT SQ Oitmaa *et al* (1991)	0.64(3)	0.096(6)	0.318(4)	1.25(2)	
	Three-dimensional Ising model				
HT BCC Butera and Comi (1997)	0.6308(5)			1.2384(6)	
MC Hasenbusch (1999)	0.6296(3)(4)			1.2367(11)	
	Field theory				
Guida and Zinn-Justin (1998)	0.6304(13)	0.109(4)	0.3258(14)	1.2396(13)	

and have estimated

$$A_0 = 0.35(2) \tag{4.3}$$

which can be compared with a previous estimate of 0.39 by Henkel (1987). It should be possible to predict this amplitude from Landau–Ginzburg effective field theory.

We have chosen to extrapolate finite-lattice sequences calculated from observables at the pseudo-critical point for each lattice pair. This technique has the advantage that it is 'unbiased', in that it does not depend on the final estimate of the bulk critical point. An alternative approach is to calculate all quantities at the estimated bulk critical point, and extrapolate those sequences instead. This has been advocated by de Quieroz (1995), for example, who claims an order of magnitude improvement in accuracy using this technique. We found no great increase in accuracy using the technique in the present case.

An extension to 7×7 sites of these exact diagonalization calculations is hardly feasible at the present time, but there are some very precise approximate methods now available, such as the DMRG (White 1992, de Jongh and van Leeuwen 2000) and path integral Monte Carlo techniques (Sandvik 1992). These might well be able to extend the results to larger lattice sizes, and allow much-improved finite-size scaling estimates of the critical parameters. They could also confirm whether or not the Casimir energy scales as in equation (4.2). Our exact diagonalization results should provide a useful calibration for such studies. We look forward to seeing such calculations in the future.

We have chosen here to work on the square lattice, rather than the triangular one, because the Hamiltonian matrix is somewhat smaller and the leading finite-size corrections are expected to be much the same for both lattices. There are, however, some hints of irregularity or alternating behaviour in some of the square lattice sequences. It might well be that the triangular lattice results are smoother.

Acknowledgments

The author would like to thank Dr P F Price and Professor I Affleck for useful discussions. Part of this work was carried out while on study leave at the Institute for Theoretical Physics, University of California at Santa Barbara, and at the Centre for Nonlinear Studies, Los Alamos National Laboratory. The author would like to thank Professor R Singh and the

organizers of the Workshop on 'Magnetic Materials in Novel Materials and Geometries' for their hospitality in Santa Barbara, and Dr J Gubernatis for his kind hospitality in Los Alamos. The calculations were performed using facilities at the New South Wales Centre for Parallel Computing, and at the Centre for Nonlinear Studies, Los Alamos. The author is very grateful to Professor R Standish and Mr D Neal for their assistance in this regard. This research was supported in part by the National Science Foundation under grant no PHY94-07194, and also by a grant from the Australian Research Council.

Appendix

The finite-size scaling amplitude for the ground-state energy (Casimir amplitude) can be calculated for free fields as follows.

A.1. Free-boson case

The zero-point energy of a free-boson field is given in d space dimensions by

$$E_0 = \tfrac{1}{2}\sum_k \omega_k \tag{A.1}$$

i.e. $\omega_k/2$ for each momentum mode. On a lattice, the free-particle Hamiltonian can be written in a finite-difference form

$$H = \frac{1}{2}\sum_{\boldsymbol{n}}\left[\dot{\phi}^2(\boldsymbol{n}) + \sum_{i=1}^{d}\left(\frac{\phi(\boldsymbol{n}+\boldsymbol{i}) - \phi(\boldsymbol{n}-\boldsymbol{i})}{2}\right)^2\right] \tag{A.2}$$

where the lattice spacing has been set to 1. The eigenmodes are plane waves

$$\phi(\boldsymbol{n}, t) = \frac{1}{N^{1/2}}\sum_{\boldsymbol{k}}[a_k \mathrm{e}^{\mathrm{i}(\boldsymbol{k}\cdot\boldsymbol{n}-\omega_k t)} + a_k^{\dagger}\mathrm{e}^{-\mathrm{i}(\boldsymbol{k}\cdot\boldsymbol{n}-\omega_k t)}] \tag{A.3}$$

where

$$\omega_k = \left[2\sum_{i=1}^{d}(1-\cos k_i)\right]^{1/2} \tag{A.4}$$

and for periodic boundary conditions the allowed momenta are

$$k_i = \frac{2\pi}{L}l_i \qquad l_i = 0, 1, 2, \ldots \tag{A.5}$$

for a lattice of $N = L^d$ sites. Hence

$$E_0 = \tfrac{1}{2}\sum_{\boldsymbol{k}}\left[2\sum_{i=1}^{d}(1-\cos k_i)\right]^{1/2} \tag{A.6}$$

i.e.

$$\epsilon_0 = \frac{1}{L^d}\sum_{\{l_i\}=0}^{L-1}\left[\sum_{i=1}^{d}\sin^2\left(\frac{\pi l_i}{L}\right)\right]^{1/2}. \tag{A.7}$$

Now the leading finite-size correction to this sum arises from the infrared (small momentum) behaviour of the lattice sum (Hasenfratz and Leutwyler 1990), and does not depend on the cutoff or regularization at large momentum. Thus we may approximate for our purposes

$$\epsilon_0 \simeq \frac{1}{L^d}\sum_{\{l_i\}=-\infty}^{\infty}\left[\sum_{i=1}^{d}\left(\frac{\pi l_i}{L}\right)^2\right]^{1/2}. \tag{A.8}$$

Now we use the Poisson resummation formula

$$\sum_{\boldsymbol{m}=-\infty}^{+\infty} f(\boldsymbol{m}L) = \frac{1}{L^d} \sum_{\boldsymbol{n}=-\infty}^{+\infty} g\left(\frac{2\pi \boldsymbol{n}}{L}\right) \tag{A.9}$$

with

$$g(\boldsymbol{k}) = \int_{-\infty}^{+\infty} \mathrm{e}^{\mathrm{i}\boldsymbol{k}\cdot\boldsymbol{x}} f(\boldsymbol{x})\, \mathrm{d}^d x \tag{A.10}$$

to show

$$\epsilon_0' = \frac{1}{4\pi} \sum_{\{m_i\}'=-\infty}^{+\infty} \int_0^\infty k^d \,\mathrm{d}k\, \frac{J_{d/2-1}(kx)}{(2\pi kx)^{d/2-1}} \qquad (x = L|\boldsymbol{m}|) \tag{A.11}$$

$$= -\frac{\Gamma(\frac{d+1}{2})}{2\pi^{\frac{d+1}{2}} L^{d+1}} \sum_{\{m_i\}'=-\infty}^{+\infty} \frac{1}{|\boldsymbol{m}|^{d+1}}. \tag{A.12}$$

The dash here implies removal of the term $\boldsymbol{m} = 0$, which corresponds to the (infinite, non-universal) *bulk* ground-state energy per site, which we simply drop.

The sum involved here is a generalization of the Riemann zeta function. It gives

$$\epsilon_0' = -\frac{A_0}{L^{d+1}} \tag{A.13}$$

where for $d = 1$, A_0 is easily evaluated

$$A_0 = \frac{\pi}{6} = 0.5236, \tag{A.14}$$

the result being familiar from conformal field theory. For higher dimensions, we have evaluated the sum numerically

$$d = 2 : A_0 = 0.7189 \tag{A.15}$$

$$d = 3 : A_0 = 0.8375. \tag{A.16}$$

The result for $d = 2$ was given previously by Hasenfratz and Niedermayer (1993).

A.2. Free-fermion case

A similar naive argument can be given for the case of a single species of free Weyl (spinless) fermions. The filled Dirac sea has energy

$$E_0 = -\sum_k \omega_k \tag{A.17}$$

where again

$$\omega_k = \left[2\sum_{i=1}^{d}(1 - \cos k_i)\right]^{1/2} \tag{A.18}$$

and we assume antiperiodic boundary conditions for the fermions

$$k_i = \frac{\pi}{L}(2l_i + 1) \qquad l_i = 0, 1, 2, \ldots. \tag{A.19}$$

Hence

$$\epsilon_0 \simeq -\frac{1}{L^d} \sum_{\{l_i\}=-\infty}^{\infty} \left[\sum_{i=1}^{d} \left(\frac{\pi(2l_i + 1)}{2L}\right)^2\right]^{1/2}. \tag{A.20}$$

We use the Poisson resummation formula again to find

$$\epsilon_0' = -\frac{1}{4\pi} \sum_{\{m_i\}'=-\infty}^{+\infty} (-1)^{\sum_i m_i} \int_0^\infty k^d \, \mathrm{d}k \, \frac{J_{d/2-1}(kx)}{(2\pi kx)^{d/2-1}} \qquad (x = L|\boldsymbol{m}|) \tag{A.21}$$

$$= \frac{\Gamma(\frac{d+1}{2})}{2\pi^{\frac{d+1}{2}} L^{d+1}} \sum_{\{m_i\}'=-\infty}^{+\infty} \frac{(-1)^{\sum_i m_i}}{|\boldsymbol{m}|^{d+1}}. \tag{A.22}$$

For $d = 1$, A_0 is easily evaluated to give

$$A_0 = \frac{\pi}{12} = 0.2618 \tag{A.23}$$

which is also familiar from conformal field theory; while for higher dimensions, we find numerically

$$d = 2 : A_0 = 0.2106 \tag{A.24}$$

$$d = 3 : A_0 = 0.1957. \tag{A.25}$$

These numbers have not been obtained previously, as far as we are aware.

References

Barber M N 1983 *Phase Transitions and Critical Phenomena* vol 8, ed C Domb and J Lebowitz (New York: Academic)

Barber M N and Hamer C J 1982 *J. Aust. Math. Soc.* B **23** 229

Bulirsch R and Stoer J 1964 *Numer. Math.* **6** 413

Butera P and Comi M 1997 *Phys. Rev.* B **56** 8212

Cardy J L 1985 *J. Phys. A: Math. Gen.* **18** L757

de Jongh M S L de C and van Leeuwen J M J 2000 *Los Alamos preprint* cond-mat/9709103

de Quieroz S L A 1995 *J. Phys. A: Math. Gen.* **27** L363

Fradkin E and Susskind L 1978 *Phys. Rev.* D **17** 2637

Guida R and Zinn-Justin J 1998 *J. Phys. A: Math. Gen.* **31** 8103

Guttman A J 1989 *Phase Transitions and Critical Phenomena* vol 13, ed C Domb and J Lebowitz (New York: Academic)

Hamer C J 1982 *J. Phys. A: Math. Gen.* **15** L675

——1983 *J. Phys. A: Math. Gen.* **16** 1257

Hamer C J and Guttmann A J 1989 *J. Phys. A: Math. Gen.* **22** 3653

Hamer C J and Irving A C 1984 *J. Phys. A: Math. Gen.* **17** 1649

Hamer C J and Johnson C H J 1986 *J. Phys. A: Math. Gen.* **19** 423

Hasenbusch M 1999 *J. Phys. A: Math. Gen.* **32** 4851

Hasenfratz P and Leutwyler H 1990 *Nucl. Phys.* B **343** 241

Hasenfratz P and Niedermayer F 1993 *Z. Phys.* B **92** 91

He H-X, Hamer C J and Oitmaa J 1990 *J. Phys. A: Math. Gen.* **23** 1775

Henkel M 1984 *J. Phys. A: Math. Gen.* **17** L795

——1986 *J. Phys. A: Math. Gen.* **19** L247

——1987 *J. Phys. A: Math. Gen.* **20** 3969

——1990 *Finite-Size Scaling and Numerical Simulation of Statistical Systems* ed V Privman (Singapore: World Scientific)

Henkel M and Patkos A 1987 *J. Phys. A: Math. Gen.* **20** 2199

Henkel M and Schütz G 1988 *J. Phys. A: Math. Gen.* **21** 2617

Lin H Q 1990 *Phys. Rev.* B **42** 6561

Lubkin S 1952 *J. Res. NBS* **48** 228

Marland L G 1981 *J. Phys. A: Math. Gen.* **14** 2047

Mon K K 1985 *Phys. Rev. Lett.* **54** 2671

Nightingale M P, Visvanath V S and Müller G 1993 *Phys. Rev.* B **48** 7696

Oitmaa J, Hamer C J and Zheng W-H 1991 *J. Phys. A: Math. Gen.* **24** 2863

Pfeuty P and Elliott R J 1971 *J. Phys. C: Solid State Phys.* **4** 2370

Price P F, Hamer C J and O'Shaughnessy D 1993 *J. Phys. A: Math. Gen.* **26** 2855

Privman V and Fisher M E 1984 *Phys. Rev.* B **30** 322
Roomany H and Wyld H W 1980 *Phys. Rev.* D **21** 3341
Sandvik A W 1992 *J. Phys. A: Math. Gen.* **25** 3667
Schulz H J, Ziman T A L and Poilblanc D 1996 *J. Physique* I **6** 675
Smith D A and Ford W F 1982 *Math. Comput.* **38** 481
Suzuki M 1976 *Prog. Theor. Phys.* **56** 1454
Uzelac K 1980 *Thesis* Orsay
van den Broeck J-M and Schwartz L W 1979 *SIAM J. Math. Anal.* **10** 658
Weigel M and Janke W 1999 *Phys. Rev. Lett.* **82** 2318
Weston R A 1990 *Phys. Lett.* B **248** 340
White S R 1992 *Phys. Rev. Lett.* **69** 2863
Yanase A, Takeshige Y and Suzuki M 1976 *J. Phys. Soc. Japan* **41** 1108
Yang C N 1952 *Phys. Rev.* **85** 808